Demonstration of Flexible mm-Wave Digital Beamforming Transmitter Using Sigma-Delta Radio-over-Fiber Link

(article starts on next page)

Demonstration of Flexible mmWave Digital Beamforming Transmitter using Sigma-Delta Radio-Over-Fiber Link

Husileng Bao[#1], Zhongxia Simon He[#2], Filippo Ponzini[*3], Christian Fager[#4]

[#]MC2, Chalmers University of Technology, Sweden
[*]GFTL ER HDE Optical Systems, Ericsson, Italy
{[1]husileng, [2]zhongxia, [4]christian.fager}@chalmers.se, [3]filippo.ponzini@ericsson.com

Abstract — **This work demonstrates a millimeter-wave digital beamforming transmitter based on a sigma-delta radio-over-fiber link. The digital beamforming is controlled from a central unit and distributed to a remote radio unit using a standardized quad small form-factor pluggable 28 (QSFP28) fiber connection. The experimental results demonstrate 26.2 GHz transmission with high-quality beamforming functionality up to 130 MHz effective radio bandwidth at 2.2 m wireless distance. The solution offers a flexible transmitter solution suitable for millimeter-wave distributed active antenna systems.**

Keywords — **mmWave, beamforming, sigma-delta modulation, radio-over-fiber, central unit.**

I. INTRODUCTION

The 3GPP frequency range 2 (FR2) for 5G is a millimeter-wave (mmWave) frequency band that offers broader bandwidth and greater data throughput than the lower bands [1]. However, the mmWave signal suffer from weak penetration and high propagation loss [2], which both limit the available communication capacity in practice. Distributed multiple-input-multiple-output (D-MIMO) offers a more uniform capacity to users, which has been shown both theoretically [3] and experimentally [4], and is therefore an attractive solution for enhanced mm-wave communication performance.

Radio-over-fiber (RoF) is already a mature technology used for implementation of distributed antenna systems in (long-term evolution) LTE communication systems, and recently for mmWave 5G [5]. Analog beamforming has been studied for a single link analog RoF (ARoF) system in [6] and the highly complex ARoF D-MIMO commercial system in [7]. Furthermore, optical beamforming solutions have been proposed to implement remote beamforming from central-unit (CU) and to simplify the remote radio unit (RRU) hardware complexity [8] [9]. Nevertheless, the solution proposed in [8] can only support a fixed beam direction by allocating a specific optical wavelength. At the same time, the solution in [9] controls the beam direction by utilizing lots of optical components. Recently, a sigma-delta-over-fiber (SDoF) based digital RoF system was proposed in [10]. Results with two remote mm-wave RRUs was presented, but beamforming or MIMO functionality was not presented.

In this paper, we investigate a novel CU-controlled mmWave SDoF architecture with digital beamforming capability. Specifically, the CU utilizes SDM techniques to generate four independent, yet fully coherent, IF bitstreams which are fed to the RRU using the four channels of a commercial quad small form-factor pluggable 28 (QSFP28) optical link. The RRU recovers the four IF signals through bandpass filtering, and without the need for any digital-analog converter (DAC). Commercial upconversion mixers are used to generate four mm-wave signals that feed a linear array antenna. In this way, the timing and coherency between the channels is accurately controlled by the CU. The experimental results verify the signal power level at each stage and demonstrate high-quality beamforming functionality up to 130 MHz effective radio bandwidth at 2.2 m wireless distance. This demonstration also can form the basis for the realization of a fully digital D-MIMO transmitter system in the future.

This paper is structured as follows: Section II explains the link architecture. Section III discusses measurement results. Finally, conclusions are drawn in Section IV.

II. LINK ARCHITECTURE

This section describes the hardware structure and the signal processing for the proposed link architecture.

A. Hardware Structure

The first part of the SDoF digital beamforming system is the CU as shown in Fig. 1. The CU includes a PC (personal computer) with Matlab for offline signal processing. The TX function generates four baseband (BB) signals, and upsamples the BB signals to 25 Gsps sample rate. The BB signals are digitally upconverted to an intermediate frequency of 2 GHz. The bandpass SDM [11] is used to generate four bitstreams at 25 Gbps data rate. Finally, the data is uploaded to the FPGA memory.

A commercial QSFP28 optical fiber link connects the FPGA to the RRU as Fig. 1. There are four parallel upconversion mixers (Analog Devices ADMV-1013) in the RRU. The mixer is able to output frequencies from 24 to 44 GHz. A 90° hybrid is used to feed the mixer with a quadrature IF signal, which is needed for single sideband upconversion. The 90° hybrid and the mixer input work as a bandpass filter to recover analog IF signal from the SDM signal. Moreover, the mixer requires a local oscillation
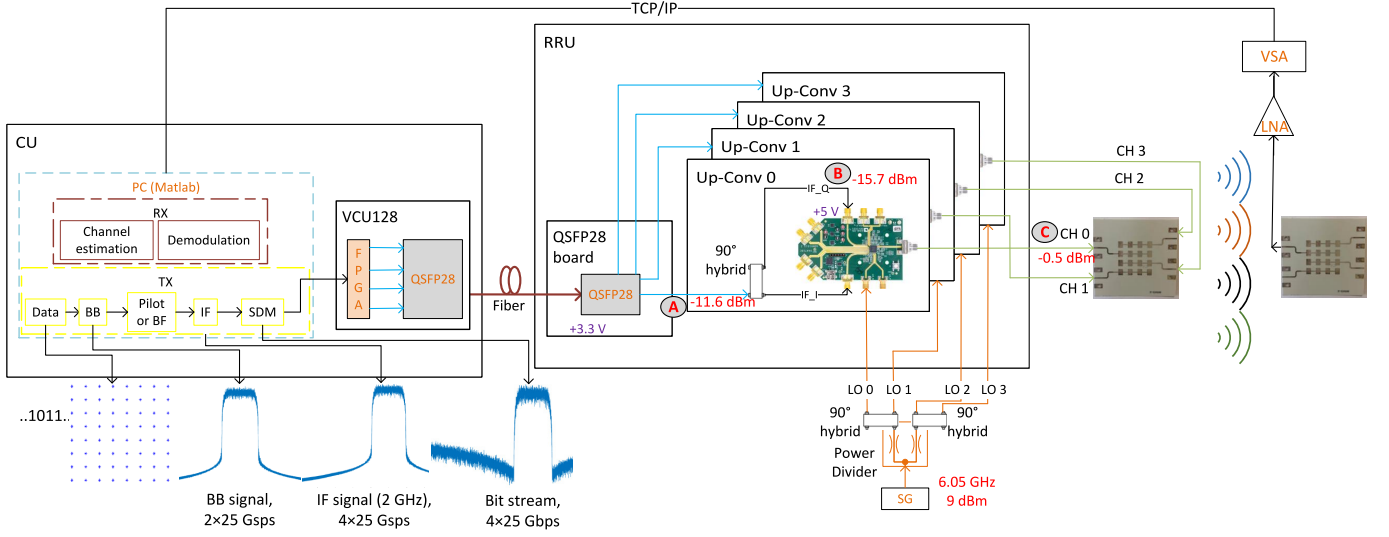
Fig. 1. The link architecture of the demonstration. At CU, the PC and FPGA generate the SDM signal to the optical fiber. The QSFP28 connected RRU has four parallel upconversions to radiate signal through a linear array patch antenna.

(LO) signal to upconvert the IF signal. Therefore a signal generator, power divider, and 90° hybrids promise coherent LO signals for the four mixers. The mixer has a built in LO quadrupler, which in combination with a 6.05 GHz LO frequency upconverts the 2 GHz IF signal to 26.2 GHz frequency.

The transmit (TX) antenna is a linear array patch antenna and has four independent feeding ports that is connected with the four mixers of the RRU. Each row of the antenna has four fixed patch elements. The receive (RX) antenna is identical to the TX antenna, but with one of the rows connected to a low noise amplifier (LNA) and VSA (vector signal analyzer, Keysight N9030A). The VSA downconverts the received mmWave signal and samples it to digital baseband data for Matlab RX signal processing.

B. Signal Processing

In our experiments, the first signal processing stage is the channel estimation while the digital beamforming is the second stage. At the channel estimation stage, the CU generates pilot signals to the RRU and TX antenna. An N-sample orthogonal pilot signal, $\mathbf{X}$, is generated by having one channel transmitting at a time:

$$\mathbf{X} = \begin{bmatrix} \mathbf{x}_0 & \mathbf{0} & \mathbf{0} & \mathbf{0} \\ \mathbf{0} & \mathbf{x}_1 & \mathbf{0} & \mathbf{0} \\ \mathbf{0} & \mathbf{0} & \mathbf{x}_2 & \mathbf{0} \\ \mathbf{0} & \mathbf{0} & \mathbf{0} & \mathbf{x}_3 \end{bmatrix}_{N \times 4}, \quad (1)$$

where $\mathbf{x}_0$, $\mathbf{x}_1$, $\mathbf{x}_2$, $\mathbf{x}_3$ are the individual channel pilot sequences. These and $\mathbf{0}$ all have a dimension of $N/4 \times 1$.

The least square channel estimation is given by as:

$$\widehat{\mathbf{h}} = \left(\mathbf{X}^{\mathrm{T}}\mathbf{X}\right)^{-1}\mathbf{X}^{\mathrm{T}}\mathbf{y}, \quad (2)$$

where $\mathbf{y}$ is the received time aligned signal of dimension $N \times 1$. $\widehat{\mathbf{h}} = \begin{bmatrix} \widehat{h}_0 & \widehat{h}_1 & \widehat{h}_2 & \widehat{h}_3 \end{bmatrix}^{\mathrm{T}}$ is the estimated 4×1 channel

vector. In our work, we have used Moore–Penrose inverse of the estimated channel matrix $\widehat{\mathbf{h}}$ to calculate the beamforming precoder $\mathbf{p}_{\mathrm{BF}}$ as:

$$\mathbf{p}_{\mathrm{ZF}} = \left(\widehat{\mathbf{h}}\widehat{\mathbf{h}}^*\right)^{-1}\widehat{\mathbf{h}} \quad (3)$$

$$\mathbf{p}_{\mathrm{BF}} = \mathbf{e}^{\mathbf{j}\angle \mathbf{p}_{\mathrm{ZF}}} \quad (4)$$

$$\mathbf{S} = \mathbf{u}\mathbf{p}_{\mathrm{BF}}^{\mathrm{T}}. \quad (5)$$

To superimpose the four signals at the receiver antenna constructively, the beamforming precoder $\mathbf{p}_{\mathrm{BF}}$ processes user data $\mathbf{u}$ according to (5) to generate the four channel signals $\mathbf{S}$.

III. MEASUREMENT RESULTS

The proposed link architecture has been implemented and experimentally evaluated using the setup in Fig. 2. The transmitter performance is first evaluated and then over-the-air experiments are performed to investigate the digital beamforming functionality in a single link application.
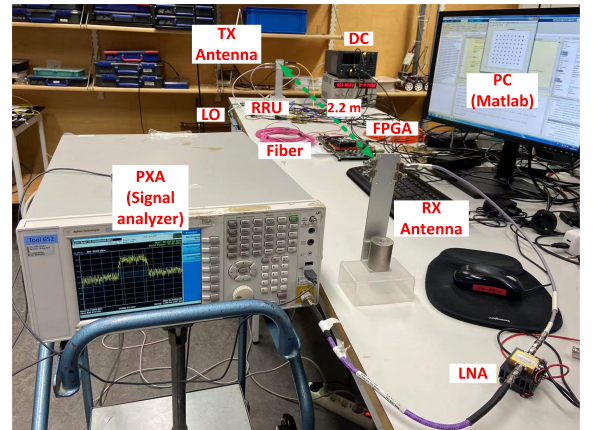

Fig. 2. The experimental setup used to demonstrate the proposed link architecture. The TX antenna is placed at 2.2 m distance from the RX antenna.

A. Power Levels

The output power limits the wireless transmission distance [12]. Therefore, this subsection investigates the power level at each stage in the proposed link architecture. The IF power generated at each of the QSFP28 output channels is measured at position A in Fig. 1. The band power at position A is -11.6 dBm. Accounting for the 90° hybrid loss, SMA connector loss, and coaxial cable loss, the IF power has dropped to -15.7 dBm at position B in Fig. 1. The active mixer has 15.2 dB gain, resulting in -0.5 dBm in-band output power for the mmWave signal at position C. It is worth noting that the power mentioned above is the average power. The peak power is higher than the average power due to the modulated communication signal's peak-to-average power ratio (PAPR).

In Fig. 3, the signal spectrum at position C of Fig. 1 shows an adjacent channel power ratio (ACPR) of 36.7 dB. Although not shown in the figure, the out-of-band spectrum is at least 25 dB below the in-band signal also far from the carrier frequency.
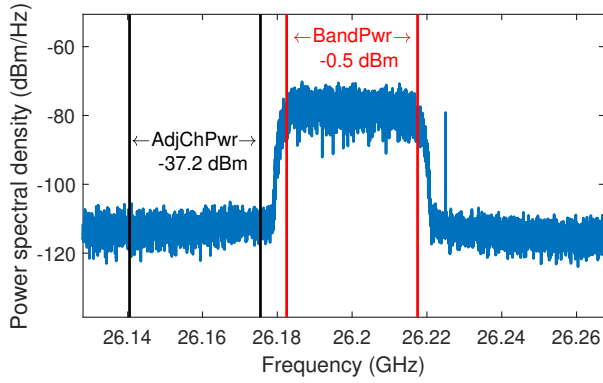

Fig. 3. The signal spectrum at position C of Fig. 1. The band power (BandPwr) is -0.5 dBm at each port of the antenna element. The adjacent channel power (AdjChPwr) is -37.2 dBm. The single tone at the right of the band power is a carrier offset signal used for receiver frequency synchronization.

B. Bandwidth Performance

In our measurements, we demonstrate digital beamforming with the SDoF system up to 130 MHz bandwidth, which is limited by the instrument available.

The normalized mean square error (NMSE) is used to quantify the signal quality. In Fig. 4, the bottom curve is the simulation (Sim) results as a benchmark for the measurements. In general, all measurement results have a similar trend as the simulated results. At 35 MHz bandwidth, the NMSE in position C is higher than at positions A and B. This slight difference is from the mixer's noise figure and the VSA's higher noise floor at 26.2 GHz. At 130 MHz, the NMSE in positions A, B, C is almost identical, which means that the performance limitations are set by the signal generated in FPGA and QSFP28 parts of the system for broader bandwidths. In conclusion, RRU does not introduce critical performance degradation but the majority of the distortion is introduced by the FPGA and/or QSFP28 components. This is in line with the observations made in [13].

C. OTA and Beamforming Performance

The RX and TX antennas have a 2.2 m distance and are mounted on identical mechanical structures during the OTA measurements, as shown in Fig. 2. The active row of the RX array antenna has the same height as CH0 of the TX antenna. Due to the propagation loss at 2.2 m distance, single channel OTA measurement result becomes noise limited and therefore has the worst NMSE in Fig. 4. However, thanks to the digital beamforming solution, the NMSE is improved and becomes close to the performance of the TX in position C. At 130 MHz bandwidth, the ideal simulated performance is -52 dB, which is 18 dB better than the measurements. This shows that the performance is limited by the hardware rather than the SDM quantization. Based on these results, we predict that the proposed transmitter architecture could support at least 500 MHz bandwidth with good performance.
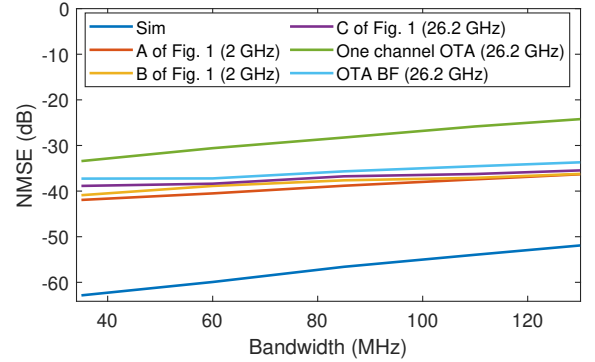

Fig. 4. Bandwidth performance analysis of the transmitter and OTA. The NMSE for an ideal SDM simulation is included as a reference (Sim). The NMSE results are measured at the positions A, B, and C in Fig. 1. OTA (26.2 GHz) with single channel (CH0) transmission is shown in the top trace (green).
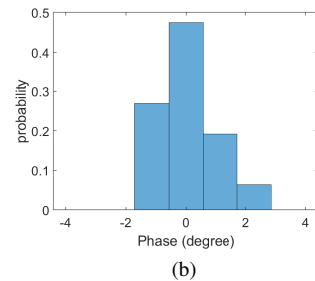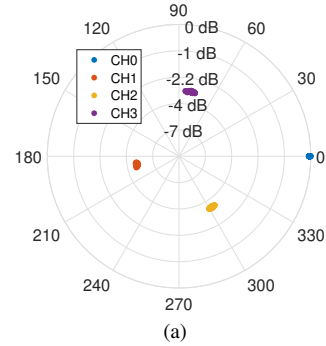

(a)

(b)

Fig. 5. The channel estimation results from 225 repeated OTA measurements. (a) Polar plot of channel information for the four channels; (b) Histogram of channel estimate variations.

Table 1. Comparison with the state-of-the-art beamforming RoF publications.

Ref.	RoF	Beamforming	Bandwidth	Modulation	OTA distance	Carrier frequency	NMSE
[6]	ARoF	Analog	1.96 GHz	16 QAM OFDM	2.2 m	28 GHz	-14 dB[a]
[7]	ARoF	Analog	1 GHz	64 QAM OFDM	10 m	28 GHz	-24.3 dB
[8]	ARoF	Analog + Optical	100 MHz	64 QAM OFDM	6.3 m	28 GHz	-31.3 dB
[9]	ARoF	Analog + Optical	3.5 GHz	16 QAM	0.5 m	60 GHz	-19.6 dB
[10]	SDoF	No	160.32 MHz	64 QAM OFDM	2.0 m	> 24 GHz	-24.4 dB
This work	SDoF	Digital	130 MHz	64 QAM	2.2 m	26.2 GHz	-33.4 dB

[a] The paper reached the bit-error-rate (BER) limit corresponding to forward error corrections (FEC) with 25% overhead. The NMSE requirement for this BER limit is 14 dB.

The digital beamforming helps to compensate for the propagation loss and is dependent on estimated channel information, as illustrated in Section II.B. Hence, channel information stability is essential. The polar plot in Fig. 5a presents the channel coefficients from 225 repeated OTA measurements, normalized to the phase and amplitude of the channel between the receiver and CH0. The normalized {amplitude, phase} of the remaining channels CH1/CH2/CH3 is given by {-4.85 dB, 191°}/{-3.37 dB, 303°}/{-3.04 dB, 79°}, respectively. These channel coefficients agree with the physical arrangement, as the CH2 and CH3 are closer to CH0 than CH1. Fig. 5b, presents a histogram for the phase variations of all channel coefficients. Almost 48% of the phase variations is between -1° and 1° with a 2.3° standard deviation. In conclusion, this demonstration promises stable channel information estimation as well as precise beamforming stability.

IV. CONCLUSION

This paper proposes a mmWave digital beamforming transmitter based on an SDoF link. The experimental results successfully demonstrate mmWave, 26 GHz, transmission of a 130 MHz wideband signal across 2.2 m wireless distance with -33.4 dB NMSE. The demonstrated bandwidth is limited by the receiver instrument, but is predicted to exceed 500 MHz. Furthermore, the results show that the transmitter can offer very stable channel information, making it is well suited for high performance digital beamforming experiments. The comparison with the state-of-the-art beamforming RoF publications in Table 1 concludes that this work is the first CU-controlled digital beamforming SDoF solution. The proposed link architecture can form the basis for realization of high performance mmWave distributed MIMO systems in the future.

ACKNOWLEDGMENT

REFERENCES

[1] J. G. Andrews, S. Buzzi, W. Choi, S. V. Hanly, A. Lozano, A. C. Soong, and J. C. Zhang, "What Will 5G Be?" *IEEE Journal on selected areas in communications*, vol. 32, no. 6, pp. 1065–1082, 2014.

[2] W. Feng, Y. Wang, D. Lin, N. Ge, J. Lu, and S. Li, "When mmWave Communications Meet Metwork Densification: A Scalable Interference Coordination Perspective," *IEEE Journal on Selected Areas in Communications*, vol. 35, no. 7, pp. 1459–1471, 2017.

[3] Z. Liu and L. Dai, "Asymptotic capacity analysis of downlink mimo systems with co-located and distributed antennas," in *2013 IEEE 24th Annual International Symposium on Personal, Indoor, and Mobile Radio Communications (PIMRC).* IEEE, 2013, pp. 1286–1290.

[4] C. Fager, S. Rimborg, E. Rådahl, H. Bao, and T. Eriksson, "Comparison of Co-located and Distributed MIMO for Indoor Wireless Communication," in *2022 IEEE Radio and Wireless Symposium (RWS)*, 2022, pp. 83–85.

[5] I. Chih-Lin, H. Li, J. Korhonen, J. Huang, and L. Han, "RAN Revolution With NGFI (xhaul) for 5G," *Journal of Lightwave Technology*, vol. 36, no. 2, pp. 541–550, 2017.

[6] D. Konstantinou, T. A. Bressner, S. Rommel, U. Johannsen, M. N. Johansson, M. V. Ivashina, A. B. Smolders, and I. T. Monroy, "5G RAN architecture based on analog radio-over-fiber fronthaul over UDWDM-PON and phased array fed reflector antennas," *Optics Communications*, vol. 454, p. 124464, 2020.

[7] M. Sung, J. Kim, E.-S. Kim, S.-H. Cho, Y.-J. Won, B.-C. Lim, S.-Y. Pyun, H. Lee, J. K. Lee, and J. H. Lee, "RoF-Based Radio Access Network for 5G Mobile Communication Systems in 28 GHz Millimeter-Wave," *Journal of Lightwave Technology*, vol. 38, no. 2, pp. 409–420, 2020.

[8] K. Ito, M. Suga, T. Arai, Y. Shirato, N. Kita, and T. Onizawa, "Passive beamformer based remote beamforming scheme for radio-over-fiber systems: Experimental demonstration using 28-GHz band reflectarray," *Optics Communications*, vol. 513, p. 128026, 2022.

[9] T. Nagayama, S. Akiba, T. Tomura, and J. Hirokawa, "Photonics-Based Millimeter-Wave Band Remote Beamforming of Array-Antenna Integrated With Photodiode Using Variable Optical Delay Line and Attenuator," *Journal of Lightwave Technology*, vol. 36, no. 19, pp. 4416–4422, 2018.

[10] C.-Y. Wu, H. Li, J. Van Kerrebrouck, A. Vandierendonck, I. L. de Paula, L. Breyne, O. Caytan, S. Lemey, H. Rogier, J. Bauwelinck *et al.*, "Distributed Antenna System Using Sigma-Delta Intermediate-Frequency-Over-Fiber for Frequency Bands Above 24 GHz," *Journal of Lightwave Technology*, vol. 38, no. 10, pp. 2765–2773, 2020.

[11] R. Schreier, G. C. Temes *et al.*, *Understanding Delta-Sigma Data Converters.* Piscataway, NJ: IEEE press, 2005, vol. 74.

[12] D. M. Pozar, *Microwave and RF Design of Wireless Systems.* John Wiley & Sons, 2000.

[13] I. C. Sezgin, M. Dahlgren, T. Eriksson, M. Coldrey, C. Larsson, J. Gustavsson, and C. Fager, "A Low-Complexity Distributed-MIMO Testbed Based on High-Speed Sigma–Delta-Over-Fiber," *IEEE Transactions on Microwave Theory and Techniques*, vol. 67, no. 7, pp. 2861–2872, 2019.